
MICRORHEOLOGY TO PROBE SMECTIC CLUSTERS IN BENT-CORE NEMATIC LIQUID CRYSTALS

 **Sathyanarayana Paladugu**

School of Physics, University of Hyderabad, Hyderabad, India.
Department of Physics, Indian Institute of Science Education and Research (IISER) Tirupati, Tirupati, India.
sathyapaladugu@gmail.com

 **Supreet Kaur**

Department of Chemical Sciences, Indian Institute of Science Education and Research (IISER) Mohali, India.

 **Golam Mohiuddin**

Department of Chemical Sciences, Indian Institute of Science Education and Research (IISER) Mohali, India.

 **Ravi Kumar Pujala**

Department of Physics, Indian Institute of Science Education and Research (IISER) Tirupati, Tirupati, India.

 **Santanu Kumar Pal**

Department of Chemical Sciences, Indian Institute of Science Education and Research (IISER) Mohali, India.

 **Surajit Dhara**

School of Physics, University of Hyderabad, Hyderabad, India.
sdsp@uohyd.ernet.in

ABSTRACT

Many bent-core nematic liquid crystals exhibit unusual physical properties due to the presence of smectic clusters, known as “cybotactic” clusters in the nematic phase. Effect of these clusters on complex shear modulus ($G^*(\omega)$) of such liquid crystals hitherto unexplored. Here, we study flow viscosities and complex shear modulus of two asymmetric bent-core liquid crystals using microrheology technique. The results are corroborated with the measurements of curvature elastic constants. Compound with shorter hydrocarbon chain (8 OCH₃) exhibit only nematic (N) phase whereas the compound with longer chain (16 OCH₃) exhibits both nematic (N) and smectic-A (SmA) phases. Our results show that the directional shear modulus of 16 OCH₃, just above the SmA to N transition temperature is strikingly different than 8 OCH₃, owing to these smectic clusters. Thus, microrheology enables us to probe smectic clusters in bent-core nematic liquid crystals.

1 Introduction

The bent-core (BC) liquid crystals captivated the interest of many scientists as they continue to exhibit new and interesting physical properties compared to the conventional calamitic liquid crystals made of rod-like molecules^{1,2}. For example, bent-core nematic liquid crystals exhibit

negative bend-splay elastic anisotropy³⁻⁹ *i.e.* $\delta K = K_{33} - K_{11} < 0$, giant flexoelectricity¹⁰⁻¹², large rotational viscosity^{4,13-15}, and induced¹⁶, spontaneous biaxiality¹⁷⁻²³. Since the free rotation of the molecules around the bow axis is hindered, the BC molecules have strong tendency to form nano-sized smectic clusters, known as cybotactic clusters^{3,24-29}. The unusual properties, some of

them reported above have been attributed to the effect of these clusters. The size of the stable smectic clusters have been measured experimentally using Cryo-transmission electron microscopy (cryo-TEM)³⁰. These smectic clusters are expected to offer both bending modulus and layer compressional modulus that would impact on the complex shear modulus of the nematic phase. However, measurements using conventional rheological techniques, involving bulk sample would smear out their effect. Therefore, microrheological techniques, involving a very small amount of sample (typically few microlitres) are important and hitherto unexplored. In this paper, we measure flow viscosities and complex shear modulus and corroborate the results with splay and bend elastic constants of two asymmetric bent-core liquid crystals. Our study shows that microrheological measurements, using self-diffusing microparticles is a sensitive technique to investigate the smectic clusters in bent-core nematic liquid crystals.

2 Materials and Methods

2.1 Materials

Two homologous bent-core compounds, namely 8 OCH₃ and 16 OCH₃ with non-polar (–OCH₃) moieties were synthesized in our laboratory, where 8 and 16 represents the length of hydrocarbon chain R (see figure 1). The details of synthesis was reported previously by us³¹. The chemical structure of the molecules and the phase transition temperatures of the compounds are shown in figure 1. They exhibit following phase transitions in cooling: 8 OCH₃: I 150.1 °C N 66.7 °C Cr and 16 OCH₃: I 126.7 °C N 97.7 °C SmA 73.4 °C Cr, respectively.

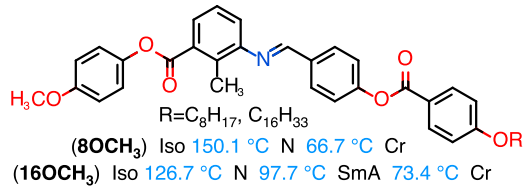


Figure 1: Chemical structure of the asymmetric bent-core molecules and phase transition temperatures.

2.2 Experimental

The experimental cells for aligning the sample were prepared with two patterned indium-tin-oxide (ITO) coated glass plates. The ITO plates were spin coated with poly-

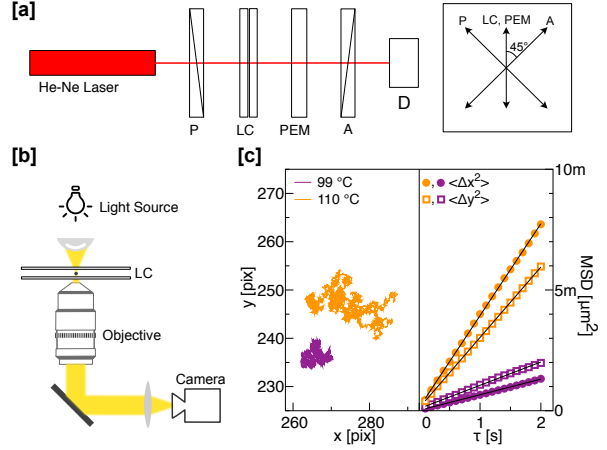


Figure 2: [a] Schematic diagram of the experimental setup for measuring birefringence, splay and bend elastic constants. [b] Setup for microrheology studies. [c] Trajectories and time evolution of MSDs of micro-particles at 99 °C and 110 °C of compound 16 OCH₃. The diffusion coefficients D_{\parallel} , D_{\perp} at 110 °C and 99 °C (in $10^{-15} \text{ m}^2/\text{s}$) are 1.90, 1.46 and 0.32, 0.48 respectively.

imide, AL1254 and baked at 180 °C for 1 h. AL1254 coated glass plates were then rubbed with a rubbing machine and assembled in antiparallel way to ensure uniform planar alignment. The glass plates were glued together with UV-curable adhesive (NOA65 - Norland Products, Inc) with silica beads as spacers. The thickness of the cells (d) were measured with interferometric method using Ocean Optics (USB4000) spectrometer and the typical cell thickness used in the study was 8 μm .

The dielectric constant, as a function of voltage (0.02 – 20 V) at different temperatures in the nematic phase, was measured at 4.111 kHz with Agilent 4980A LCR meter. The perpendicular component of dielectric constant (ϵ_{\perp}) was obtained from the measurement below the Freedericksz threshold voltage (V_{th}) and the parallel component (ϵ_{\parallel}) was obtained by extrapolating the voltage dependent dielectric constant to $V \rightarrow \infty$, *i.e.*, $1/V \rightarrow 0$. Simultaneously, the voltage dependent optical retardation was measured with the help of a home built electrooptic setup, consisting of a photo-elastic modulator (Hinds Instruments) and a lock-in amplifier (SRS-830). The experimental diagram of the setup is shown in figure 2[a]. From the Freedericksz threshold voltage (V_{th}) of the retardation measurement, the splay elastic constant (K_{11}) was measured, using the relation, $K_{11} = \epsilon_0 \Delta \epsilon (V_{\text{th}}/\pi)^2$, where $\Delta \epsilon = \epsilon_{\parallel} - \epsilon_{\perp}$ is dielectric anisotropy. The bend elastic constant (K_{33}) was obtained by fitting the voltage dependent optical retar-

dation, following the method described in Refs.^{32–34}. The accuracy in the measurement of elastic constant is within 6%.

The flow viscosities parallel (η_{\parallel}) and perpendicular (η_{\perp}) to the director were measured by measuring self-diffusion of a silica particle of diameter $3 \mu\text{m}$ ^{35,36}. Before dispersing in LCs, the particles were treated with octadecyldimethyl (3-trimethoxysilylpropyl) ammonium chloride (DMOAP), which align the director normal to the surface³⁷. Normal anchoring induces a point defect and stabilises a dipolar director field surrounding the particles as a result of which the particles are levitated in the bulk due to elastic repulsion from the surface³⁸. This is advantageous as the data collection is required for longer duration. The dynamics of the Brownian motion of an isolated silica particle in LCs was recorded through a 60X water immersion objective using a CCD camera (iDs-UI) connected to a Nikon inverted microscope with a frame rate of 20 fps³⁹. The diagram of the experimental setup is shown in the figure 2[b]. The trajectories of particles are extracted from recorded sequence of images using Python routine, known as Trackpy⁴⁰. The mean square displacements (MSD) along parallel and perpendicular to the director were measured. The diffusion coefficients parallel (D_{\parallel}) and perpendicular (D_{\perp}) to the director were measured from the respective MSDs as a function of the lag time τ , using the equations $\langle x(\tau) - x(0)^2 \rangle = 2D_{\parallel}\tau$ and $\langle y(\tau) - y(0)^2 \rangle = 2D_{\perp}\tau$. The corresponding viscosities are calculated, using the Stokes-Einstein equation, $\eta_{\parallel,\perp} = k_B T / 6\pi R D_{\parallel,\perp}$, where k_B is the Boltzmann constant, T is the absolute temperature and R is the radius of the microparticle³⁷.

The complex viscoelastic shear modulus $G^*(\omega) = G'(\omega) + iG''(\omega)$, where G' is storage modulus and G'' is loss modulus in frequency (ω) domain, was calculated using the Generalized Stokes-Einstein Equation (GSER)⁴¹. The GSER in the Fourier domain can be expressed as:

$$G^*(\omega) = G'(\omega) + iG''(\omega) = \frac{k_B T}{\pi R i \omega \mathcal{F}\{\langle \Delta r^2(t) \rangle\}} \quad (1)$$

The parallel ($G_{\parallel}^*(\omega)$) and perpendicular components ($G_{\perp}^*(\omega)$) of the complex shear modulus $G^*(\omega)$ were obtained from the MSD along parallel and perpendicular to the nematic director by the equations; $G_{\parallel}^*(\omega) = \frac{k_B T}{2\pi R i \omega \mathcal{F}\{\langle \Delta x^2(t) \rangle\}}$ and $G_{\perp}^*(\omega) = \frac{k_B T}{2\pi R i \omega \mathcal{F}\{\langle \Delta y^2(t) \rangle\}}$, respectively⁴².

3 Results and discussion

3.1 Splay and bend elastic constants

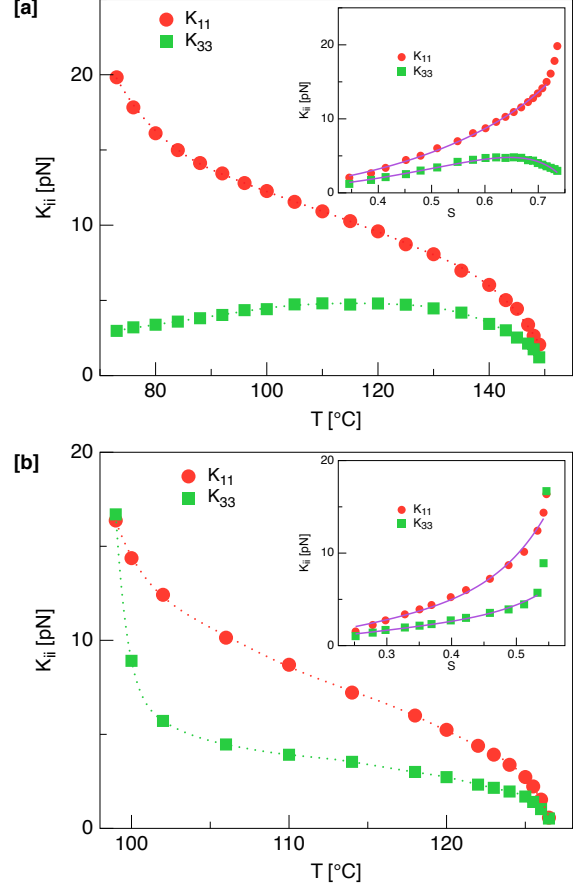


Figure 3: [a] Temperature dependent splay (K_{11}) and bend (K_{33}) elastic constants of 8 OCH₃. (inset) K_{ii} as a function of order parameter S . [b] Temperature dependent (K_{11}) and (K_{33}) of 16 OCH₃. (inset) K_{ii} as a function of order parameter S . Continuous lines are theoretical fits to equation 2.

We begin with the discussion of splay (K_{11}) and bend (K_{33}) elastic constants of the compounds. Both the compounds exhibit positive birefringence (Δn) and dielectric anisotropy ($\Delta\epsilon$) (see Supplementary Information). The temperature dependence of K_{11} and K_{33} of both the compounds is shown in figure 3[a] and 3[b]. The bend-splay anisotropy ($\delta K_{31} = K_{33} - K_{11}$) of the compound 8 OCH₃ is negative in the entire nematic range and its magnitude continues to increase with decreasing temperature. Similar negative anisotropy has been reported in many symmetric and asymmetric bent-core nematic liquid crystals^{8,9,14,43}. The negative anisotropy is attributed to the coupling of the bent-shape of the molecules with the bend distortion³. For

most liquid crystals made of rod-like molecules, $K_{ii} \propto S^2$, where S is the orientational order parameter. To see how K_{ii} of these compounds depend on the order parameter, we plot K_{ii} as a function of S and show in the inset of figure 3[a]. The order parameter S was obtained from the temperature dependent birefringence (Supplementary Information). It is noticed that K_{33} shows antagonistic dependence on the order parameter and simply can not be fitted to the second-order on S . In particular, K_{33} of 16OCH₃ tends to decrease after a pronounced maximum. The dependence of K_{ii} on S could be better explained using more detailed mean-field calculations given by Berreman and Meiboom⁴⁴. It introduces a third-order dependence on S and given by:

$$K_{ii} = K_i^{(2)} S^2 + K_i^{(3)} S^3 + K_i^{(4)} \frac{S^4}{(1-S)^2} \quad (2)$$

where K_i^n , $n = 2, 3, 4$ are fitting parameters. The continuous line in the insets of figure 3[a] is a theoretical fit to the equation 2. Considering $K_i^{(2)-(4)}$ s are temperature independent, the fitting parameters (measured in pN) are found to be $K_1^{(2)} = 14.3 \pm 1.1$, $K_1^{(3)} = 13.7 \pm 1.2$, $K_1^{(4)} = 0.7 \pm 0.1$, and $K_3^{(2)} = 6.4 \pm 1.1$, $K_3^{(3)} = 17.2 \pm 1.2$, $K_3^{(4)} = -1.8 \pm 0.1$.

Temperature dependence of K_{11} and K_{33} of the compound 16OCH₃ is shown in figure 3[b]. In this compound, the bend-splay anisotropy, $\delta K_{31} = K_{33} - K_{11}$ is also negative, except very close to the N-SmA phase transition temperature. In particular, as the N-SmA transition is approached, δK_{31} tends to change sign from negative to positive. This feature is explained by the strong pre-translational divergence of K_{33} as bend deformations are incompatible with the equidistance of smectic layers. The dependence of K_{ii} on S is shown in the inset of figure 3[b]. The excellent fits are obtained with the fit-parameters; $K_1^{(2)} = 46.5 \pm 1.1$, $K_1^{(3)} = -67.5 \pm 1.2$, $K_1^{(4)} = 26.3 \pm 0.1$ and $K_3^{(2)} = 30.9 \pm 1.1$, $K_3^{(3)} = -48.1 \pm 1.2$, $K_3^{(4)} = 10.8 \pm 0.1$.

3.2 Flow viscosities

In what follows we measure the flow viscosities of these compounds from the self-diffusion of microparticles following the technique discussed in the experimental section. The measurements are restricted only in the nematic phase as the particles tend to sediment quickly in the isotropic phase. Some representative trajectories of a microparticle and corresponding MSDs at two temperatures, namely 99

°C and 110 °C for the compound 16OCH₃ are shown in figure 2[c]. It is found that at 110 °C, $D_{||}/D_{\perp} \simeq 1.3$ whereas at 99 °C, which is very close to the N-SmA transition temperature, $D_{||}/D_{\perp} \simeq 0.7$. The temperature de-

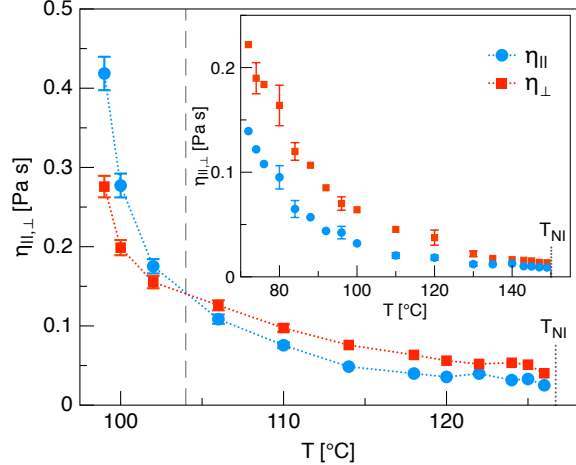


Figure 4: Temperature dependent flow viscosities coefficients parallel ($\eta_{||}$) and perpendicular (η_{\perp}) to the director of 16OCH₃. (inset) Temperature dependent ($\eta_{||}$) and perpendicular (η_{\perp}) of 8OCH₃. T_{NI} indicates isotropic to nematic phase transition temperature.

pendent viscosities parallel and perpendicular to the director, namely $\eta_{||}$, η_{\perp} of the compound 8OCH₃, below the isotropic to nematic transition temperature (T_{NI}) are shown in the inset of figure 4. Both increase with decreasing temperature as expected. It is noticed that in the entire nematic range $\eta_{\perp} > \eta_{||}$, thus viscosity anisotropy ($\delta\eta = \eta_{\perp} - \eta_{||}$) is positive. For example, at the lowest temperature ($T = 70$ °C), $\delta\eta = \eta_{\perp} - \eta_{||} \simeq 100$ mPas.

The temperature dependent viscosities of compound 16OCH₃ in the nematic phase are shown in the figure 4. Both $\eta_{||}$ and η_{\perp} increase with decreasing temperature as expected. Interestingly, it is found that below $T \approx 104$ °C, $\delta\eta$ changes sign from positive to negative. For example, at $T = 114$ °C, $\delta\eta \simeq 40$ mPas whereas at $T = 98$ °C, $\delta\eta \simeq -110$ mPas. This result can be explained as follows. The compound 16OCH₃ has cybotactic clusters in the nematic phase. These clusters are stable compared to the unstable clusters in liquid crystals with rod-like molecules as the free rotation of the former around the bow axis is reduced sufficiently due to the steric hindrance. Moreover, the size and volume fraction of these clusters near the N to SmA transition are expected to grow. The resulting smectic planes of the clusters are orient perpendicular to the director in a planar cell. These clusters effectively

reduces the self-diffusion of the microparticle along the director (perpendicular to the smectic planes) compared to the perpendicular direction (parallel to the smectic planes), resulting negative viscosity anisotropy.

3.3 Complex shear modulus

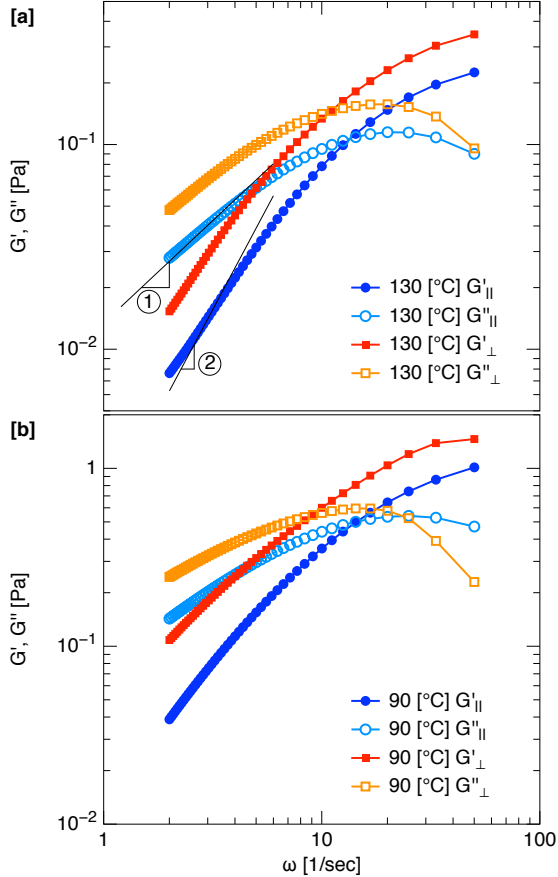


Figure 5: Frequency dependent storage ($G'(\omega)$) and loss modulus ($G''(\omega)$) of 8 OCH₃. The subscripts \parallel and \perp denote the components parallel and perpendicular to the director at (a) 130 °C and (b) 90 °C. ① and ② represents the exponents of ω corresponding to loss and storage moduli, respectively in Maxwell-fluid model.

The temperature dependent elastic constants and flow viscosities demonstrated the presence of stable cybotactic clusters in the nematic phase of compound 16 OCH₃ that contributes greatly to these properties, specially near the N to SmA phase transition. As a next step, we investigate the effect of these clusters on the complex shear modulus $G^*(\omega)$. Figure 5 and 6 shows the frequency dependence of storage ($G'_{\parallel}(\omega)$ and $G'_{\perp}(\omega)$) and loss modulus ($G''_{\parallel}(\omega)$ and $G''_{\perp}(\omega)$) along parallel and perpendicular to the ne-

matic director at two different temperatures. Overall, both parallel and perpendicular components exhibit fluid-like behaviour: storage modulus lower than the corresponding loss modulus below a critical frequency. In the low frequency range one observes a behaviour typical of a Maxwell-fluid: $G''_{\parallel,\perp}(\omega) \propto \omega$ and $G'_{\parallel,\perp}(\omega) \propto \omega^2$ (see figure 5[a] and figure 6[a]).

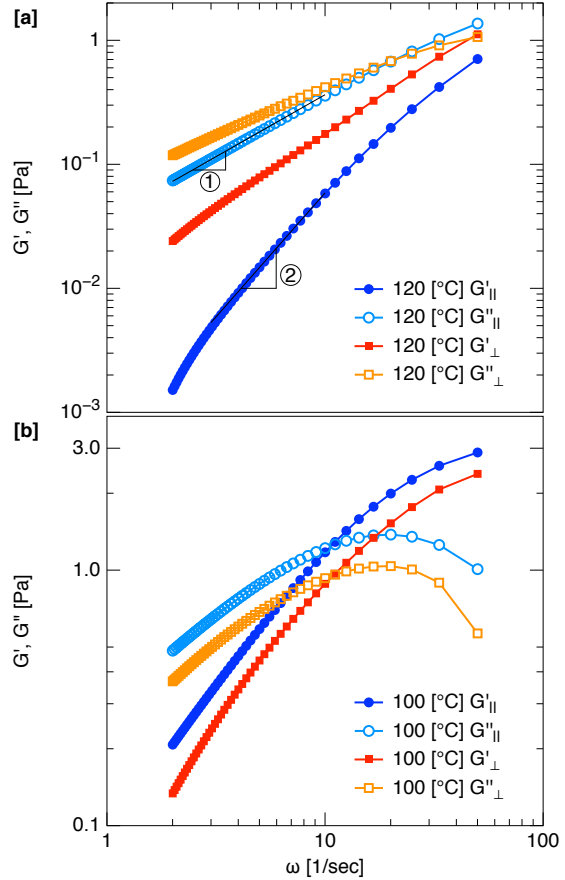


Figure 6: Frequency dependent storage ($G'(\omega)$) and loss modulus ($G''(\omega)$) of 16 OCH₃. The subscripts \parallel and \perp denote the components parallel and perpendicular to the director at (a) 120 °C and (b) 100 °C. ① and ② represents the exponents of ω corresponding to loss and storage moduli, respectively in Maxwell-fluid model.

In the nematic phase the perpendicular components are greater than the corresponding parallel components. *i.e.*, $G'_{\perp}(\omega) > G'_{\parallel}(\omega)$ and $G''_{\perp}(\omega) > G''_{\parallel}(\omega)$ (see figure 5[a],[b]). Similar behaviour is also seen in compound 16 OCH₃ at $T = 120$ °C (figure 6[a]). However, at lower temperature ($T = 100$ °C), just above the N-SmA transition temperature, the trend is quite opposite when the relative magnitudes of the parallel and perpendicular components are compared. In particular, $G'_{\parallel}(\omega) > G'_{\perp}(\omega)$

and also $G''_{\parallel}(\omega) > G''_{\perp}(\omega)$ (see figure 6[b]), which is just opposite to the behaviour seen at higher temperature ($T = 120$ °C). In addition, the magnitudes of the directional moduli at $T = 100$ °C are almost one order of magnitude larger than that measured at $T = 120$ °C. To bring out the contrasting behaviour we show the ratios $G'_{\parallel}(\omega)/G'_{\perp}(\omega)$ and $G''_{\parallel}(\omega)/G''_{\perp}(\omega)$ at a fixed ω in Table-1 and Table-2. In compound 8 OCH₃, at two different temperatures $G'_{\parallel}(\omega)/G'_{\perp}(\omega) < 1$ and $G''_{\parallel}(\omega)/G''_{\perp}(\omega) < 1$ (Table-1). For compound 16 OCH₃ at higher temperature ($T = 120$ °C), both the ratios are also less than 1 (Table-2). However, at lower temperature ($T = 100$ °C), $G'_{\parallel}(\omega)/G'_{\perp}(\omega) > 1$ and $G''_{\parallel}(\omega)/G''_{\perp}(\omega) > 1$, which is opposite to the feature observed at $T = 120$ °C. Thus, parallel components of complex viscoelastic shear modulus of 16 OCH₃ exceeds the perpendicular components just above the N-SmA phase transition temperature.

Temp [°C]	$G'_{\parallel}(\omega)/G'_{\perp}(\omega)$	$G''_{\parallel}(\omega)/G''_{\perp}(\omega)$
130	0.5	0.6
090	0.3	0.6

Table 1: Ratios of real and imaginary components along parallel and perpendicular to the director of compound 8 OCH₃ at $\omega = 2 \text{ sec}^{-1}$.

Temp [°C]	$G'_{\parallel}(\omega)/G'_{\perp}(\omega)$	$G''_{\parallel}(\omega)/G''_{\perp}(\omega)$
120	0.1	0.6
100	1.5	1.3

Table 2: Ratios of real and imaginary components along parallel and perpendicular to the director of compound 16 OCH₃ at $\omega = 2 \text{ sec}^{-1}$.

This distinct feature in the nematic phase can be explained considering the contribution of stable cybotactic clusters. In analogy with smectic droplets, the storage modulus of the clusters can be written as $G' = C\sqrt{(KB/L)}$ where K is the bending modulus, B is the layer compressional modulus, L is the cluster size and C is a constant^{45,46}. At higher temperature (near NI transition), naturally the clusters are unstable, consequently the contribution due to the layer compressional modulus B is negligible. As the temperature is reduced towards the N-SmA transition, the clusters become stable and their size and the volume fraction increases⁴⁷ as a result of which G' is enhanced. Taking $G' = 2 \text{ Pa}$ (figure 6[b]), $K = 5 \text{ pN}$ (figure 3[b]), $C \approx 0.2$ ⁴⁶ and assuming a typical layer compressional modulus $B \approx 10^6 \text{ Pa}$ ⁴⁸, the calculated cluster size $L \approx 50 \text{ nm}$, which is very close to the size measured by Cryo-

transmission electron microscopy (cryo-TEM) in similar bent-core liquid crystals³⁰.

4 Conclusions

We studied elastic properties, flow viscosities and directional shear modulus of two bent-core liquid crystals. The bend-splay anisotropy ($\delta K = K_{33} - K_{11}$) of compound 8 OCH₃ is negative at all temperatures, whereas in 16 OCH₃, δK tends to change sign just above the N-SmA transition temperature. In compound 8 OCH₃, the flow viscosity anisotropy $\delta\eta = (\eta_{\perp} - \eta_{\parallel}) > 0$, at all temperatures. In case of 16 OCH₃ it changes sign just above the N-SmA phase transition temperature. The parallel components of complex shear modulus of compound 16 OCH₃ exceeds the perpendicular components, just above the N-SmA phase transition temperature. This feature is explained considering the contribution of layer compressional modulus of stable smectic clusters in the nematic phase. Our microrheological studies provided an approximate estimate of smectic clusters size. This technique requires a few microlitres of sample and can be used for probing the effect of nanoscale heterogeneity due to short-range order in liquid crystals and in other soft materials.

References

- [1] Hideo Takezoe and Yoichi Takanishi. Bent-core liquid crystals: Their mysterious and attractive world. *Japanese Journal of Applied Physics*, 45(2A):597–625, feb 2006.
- [2] Antal Jákli, Oleg D. Lavrentovich, and Jonathan V. Selinger. Physics of liquid crystals of bent-shaped molecules. *Rev. Mod. Phys.*, 90:045004, Nov 2018.
- [3] P. Sathyanarayana, M. Mathew, Q. Li, V. S. S. Sastry, B. Kundu, K. V. Le, H. Takezoe, and Surajit Dhara. Splay bend elasticity of a bent-core nematic liquid crystal. *Phys. Rev. E*, 81:010702, Jan 2010.
- [4] P. Sathyanarayana, S. Radhika, B. K. Sadashiva, and Surajit Dhara. Structure–property correlation of a hockey stick-shaped compound exhibiting n-sma-smca phase transitions. *Soft Matter*, 8:2322–2327, 2012.
- [5] Verena Görtz, Christopher Southern, Nicholas W. Roberts, Helen F. Gleeson, and John W. Goodby.

- Unusual properties of a bent-core liquid-crystalline fluid. *Soft Matter*, 5:463–471, 2009.
- [6] Pramod Tadapatri, Uma S. Hiremath, C. V. Yelamaggad, and K. S. Krishnamurthy. Permittivity, conductivity, elasticity, and viscosity measurements in the nematic phase of a bent-core liquid crystal. *The Journal of Physical Chemistry B*, 114(5):1745–1750, 02 2010.
- [7] M. Majumdar, P. Salamon, A. Jákli, J. T. Gleeson, and S. Sprunt. Elastic constants and orientational viscosities of a bent-core nematic liquid crystal. *Phys. Rev. E*, 83:031701, Mar 2011.
- [8] S. Kaur, J. Addis, C. Greco, A. Ferrarini, V. Görtz, J. W. Goodby, and H. F. Gleeson. Understanding the distinctive elastic constants in an oxadiazole bent-core nematic liquid crystal. *Phys. Rev. E*, 86:041703, Oct 2012.
- [9] Nejmettin Avcı, Volodymyr Borshch, Dipika Deb-nath Sarkar, Rahul Deb, Gude Venkatesh, Taras Turiv, Sergij V. Shiyonovskii, Nandiraju V. S. Rao, and Oleg D. Lavrentovich. Viscoelasticity, dielectric anisotropy, and birefringence in the nematic phase of three four-ring bent-core liquid crystals with an l-shaped molecular frame. *Soft Matter*, 9:1066–1075, 2013.
- [10] J. Harden, B. Mbanda, N. Éber, K. Fodor-Csorba, S. Sprunt, J. T. Gleeson, and A. Jákli. Giant flexoelectricity of bent-core nematic liquid crystals. *Phys. Rev. Lett.*, 97:157802, Oct 2006.
- [11] P. Sathyanarayana and Surajit Dhara. Antagonistic flexoelectric response in liquid crystal mixtures of bent-core and rodlike molecules. *Phys. Rev. E*, 87:012506, Jan 2013.
- [12] Khoa Van Le, Fumito Araoka, Katalin Fodor-Csorba, Ken Ishikawa, and Hideo Takezoe. Flexoelectric effect in a bent-core mesogen. *Liquid Crystals*, 36(10-11):1119–1124, 2009.
- [13] Paladugu Sathyanarayana, Tatipamula Arun Kumar, Vanka Srinivasa Suryanarayana Sastry, Manoj Mathews, Quan Li, Hideo Takezoe, and Surajit Dhara. Rotational viscosity of a bent-core nematic liquid crystal. *Applied Physics Express*, 3(9):091702, sep 2010.
- [14] P. Sathyanarayana, V. S. R. Jampani, M. Skarabot, I. Musevic, K. V. Le, H. Takezoe, and S. Dhara. Viscoelasticity of ambient-temperature nematic binary mixtures of bent-core and rodlike molecules. *Phys. Rev. E*, 85:011702, Jan 2012.
- [15] E. Dorjgotov, K. Fodor-Csorba, J. T. Gleeson, S. Sprunt, and A. Jákli. Viscosities of a bent-core nematic liquid crystal. *Liquid Crystals*, 35(2):149–155, 2008.
- [16] J. A. Olivares, S. Stojadinovic, T. Dingemans, S. Sprunt, and A. Jákli. Optical studies of the nematic phase of an oxazole-derived bent-core liquid crystal. *Phys. Rev. E*, 68:041704, Oct 2003.
- [17] Bharat R. Acharya, Andrew Primak, and Satyendra Kumar. Biaxial nematic phase in bent-core thermotropic mesogens. *Phys. Rev. Lett.*, 92:145506, Apr 2004.
- [18] L. A. Madsen, T. J. Dingemans, M. Nakata, and E. T. Samulski. Thermotropic biaxial nematic liquid crystals. *Phys. Rev. Lett.*, 92:145505, Apr 2004.
- [19] Yun Jang, Vitaly P. Panov, Antoni Kocot, J. K. Vij, A. Lehmann, and C. Tschierske. Optical confirmation of biaxial nematic (nb) phase in a bent-core mesogen. *Applied Physics Letters*, 95(18):183304, 2009.
- [20] Ying Xiang, J. W. Goodby, V. Görtz, and H. F. Gleeson. Revealing the uniaxial to biaxial nematic liquid crystal phase transition via distinctive electroconvection. *Applied Physics Letters*, 94(19):193507, 2009.
- [21] Matthias Lehmann. Biaxial nematics from their prediction to the materials and the vicious circle of molecular design. *Liquid Crystals*, 38(11-12):1389–1405, 2011.
- [22] HyungGuen Yoon, Shin-Woong Kang, Matthias Lehmann, Jung Ok Park, Mohan Srinivasarao, and Satyendra Kumar. Homogeneous and homeotropic alignment of bent-core uniaxial and biaxial nematic liquid crystals. *Soft Matter*, 7:8770–8775, 2011.
- [23] T. B. T. To, T. J. Sluckin, and G. R. Luckhurst. Biaxiality-induced magnetic field effects in bent-core nematics: Molecular-field and Landau theory. *Phys. Rev. E*, 88:062506, Dec 2013.
- [24] P. Sathyanarayana, B. K. Sadashiva, and Surajit Dhara. Splay-bend elasticity and rotational viscosity of liquid crystal mixtures of rod-like and bent-core molecules. *Soft Matter*, 7:8556–8560, 2011.

- [25] Carsten Tschierske and Demetri J. Photinos. Biaxial nematic phases. *J. Mater. Chem.*, 20:4263–4294, 2010.
- [26] RONALD Y. DONG. Recent developments in biaxial liquid crystals: An nmr perspective. *International Journal of Modern Physics B*, 24(24):4641–4682, 2010.
- [27] Christina Keith, Anne Lehmann, Ute Baumeister, Marko Prehm, and Carsten Tschierske. Nematic phases of bent-core mesogens. *Soft Matter*, 6:1704–1721, 2010.
- [28] Oriano Francescangeli and Edward T. Samulski. Insights into the cybotactic nematic phase of bent-core molecules. *Soft Matter*, 6:2413–2420, 2010.
- [29] Valentina Domenici. Dynamics in the isotropic and nematic phases of bent-core liquid crystals: Nmr perspectives. *Soft Matter*, 7:1589–1598, 2011.
- [30] C. Zhang, M. Gao, N. Diorio, W. Weissflog, U. Baumeister, S. Sprunt, J. T. Gleeson, and A. Jákli. Direct observation of smectic layers in thermotropic liquid crystals. *Phys. Rev. Lett.*, 109:107802, Sep 2012.
- [31] Supreet Kaur, Golam Mohiuddin, Vidhika Punjani, Raj Kumar Khan, Sharmistha Ghosh, and Santanu Kumar Pal. Structural organization and molecular self-assembly of a new class of polar and non-polar four-ring based bent-core molecules. *Journal of Molecular Liquids*, 295:111687, 2019.
- [32] Heinz J. Deuling. Deformation of nematic liquid crystals in an electric field. *Molecular Crystals and Liquid Crystals*, 19(2):123–131, 1972.
- [33] Hans Gruler, Terry J. Scheffer, and Gerhard Meier. Elastic constants of nematic liquid crystals. *Zeitschrift für Naturforschung A*, 27:966, 2019-12-19T06:04:14.435+01:00 1972.
- [34] G Barbero and L R Evangelista. *An Elementary Course on the Continuum Theory for Nematic Liquid Crystals*. WORLD SCIENTIFIC, 2000.
- [35] J. C. Loudet, P. Hanusse, and P. Poulin. Stokes drag on a sphere in a nematic liquid crystal. *Science*, 306(5701):1525–1525, 2004.
- [36] Holger Stark. Physics of colloidal dispersions in nematic liquid crystals. *Physics Reports*, 351(6):387–474, 2001.
- [37] M. Škarabot and I. Muševič. Direct observation of interaction of nanoparticles in a nematic liquid crystal. *Soft Matter*, 6:5476–5481, 2010.
- [38] O. P. Pishnyak, S. Tang, J. R. Kelly, S. V. Shiyonovskii, and O. D. Lavrentovich. Levitation, lift, and bidirectional motion of colloidal particles in an electrically driven nematic liquid crystal. *Phys. Rev. Lett.*, 99:127802, Sep 2007.
- [39] John C. Crocker and David G. Grier. Methods of digital video microscopy for colloidal studies. *Journal of Colloid and Interface Science*, 179(1):298–310, 1996.
- [40] Dan Allan, Casper van der Wel, Nathan Keim, Thomas A Caswell, Devin Wieker, Ruben Verweij, Chaz Reid, Thierry, Lars Grueter, Kieran Ramos, apiszcz, zoeith, Rebecca W Perry, François Boulogne, Prashant Sinha, pfgliozzi, Nicolas Bruot, Leonardo Uieda, Jan Katins, Hadrien Mary, and Aron Ahmadi. `soft-matter/trackpy: Trackpy v0.4.2`, October 2019.
- [41] T. G. Mason, K. Ganesan, J. H. van Zanten, D. Wirtz, and S. C. Kuo. Particle tracking microrheology of complex fluids. *Phys. Rev. Lett.*, 79:3282–3285, Oct 1997.
- [42] Jun He, Michael Mak, Yifeng Liu, and Jay X. Tang. Counterion-dependent microrheological properties of *f*-actin solutions across the isotropic-nematic phase transition. *Phys. Rev. E*, 78:011908, Jul 2008.
- [43] Brindaban Kundu, R. Pratibha, and N. V. Madhusudana. Anomalous temperature dependence of elastic constants in the nematic phase of binary mixtures made of rodlike and bent-core molecules. *Phys. Rev. Lett.*, 99:247802, Dec 2007.
- [44] Dwight W. Berreman and Saul Meiboom. Tensor representation of oseen-frank strain energy in uniaxial cholesterics. *Phys. Rev. A*, 30:1955–1959, Oct 1984.
- [45] P. Panizza, D. Roux, V. Vuillaume, C.-Y. D. Lu, and M. E. Cates. Viscoelasticity of the onion phase. *Langmuir*, 12(2):248–252, 1996.
- [46] S Fujii, S Komura, Y Ishii, and C-Y D Lu. Elasticity of smectic liquid crystals with focal conic domains. *Journal of Physics: Condensed Matter*, 23(23):235105, may 2011.
- [47] Y. P. Panarin, S. P. Sreenilayam, J. K. Vij, A. Lehmann, and C. Tschierske. Formation and development of nanometer-sized cybotactic clusters in

- bent-core nematic liquid crystalline compounds. *Beilstein J. Nanotechnol.*, 9(9):1288, 2018.
- [48] M. Benzekri, T. Claverie, J. P. Marcerou, and J. C. Rouillon. Nonvanishing of the layer compressional elastic constant at the smectic-a-to-nematic phase transition: A consequence of landau-peierls instability? *Phys. Rev. Lett.*, 68:2480–2483, Apr 1992.